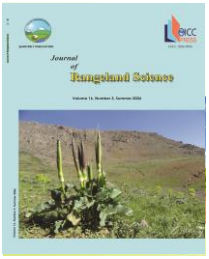

J. Rangeland Sci., 2026; 16(3): 266-277

Journal of Rangeland Science (JRS)

https://doi.org/10.57647/JRS.2026.1603.24

Research Article

# Impact of Plant Species Diversity on Aboveground Biomass and Carbon Sequestration in the Peri-Urban Rangelands of North western Tehran, Iran

Tara Mousivand[1], Zahra Azizi[2,*], Mohammad Mehdi Dehshiri[3], Lobat Taghavi[1], Mahdi Ramezani[1]

[1] *Department of Natural Resources and Environment, SR.C., Islamic Azad University, Tehran, Iran*
[2] *Department of Geoinformation and Geomatics Engineering, Shahid Beheshti University, Tehran, Iran*
[3] *Department of Natural Resources and Environment, Bo.C., Islamic Azad University, Borujerd, Iran*

*Corresponding author: zah_azizi@sbu.ac.ir

**Article History:**

Received:
14 February 2025

Revised:
12 December 2025

Accepted:
19 December 2025

Published in Issue:
30 September 2026



**Abstract**

Urban expansion is reshaping peri-urban ecosystems, including the rangelands of northwestern Tehran. This study aimed to examine whether plant species diversity enhances above-ground biomass (AGB) and, by extension, carbon storage within three rangeland sites that define the analytical area of interest (AOI). In 2022, field sampling recorded 1,558 specimens representing 38 plant species. The dominant taxa included *Bromus tectorum* and *Astragalus belgheisicus*, whereas *Henrardia persica* and *Melica persica* were rare. AGB was quantified via direct harvest and standard laboratory procedures, and organic carbon was inferred from organic matter. Diversity indices (e.g., Shannon–Wiener, Simpson, Margalef, Menhinick, Pielou) were computed. Most of the indices were positively related to AGB. Shannon ($r \approx 0.63$; $p < 0.05$) and Simpson ($r \approx 0.42$; $p < 0.05$) exhibited significant positive relations with AGB; other richness/evenness metrics showed consistent but weaker trends, whereas Hill's number showed no clear effect. Sentinel-2 (2018, 2022) imagery supported land cover mapping using supervised Maximum Likelihood Classification (MLC). Accuracy assessment was performed within the AOI, and Normalized Difference Vegetation Index (NDVI) aided vegetation characterization. Vegetation cover had decreased significantly (34%) between 2018 and 2022. Findings indicated that, within the studied rangeland AOI, higher plant diversity is related to greater AGB and carbon potential.

**Keywords:** Plant biodiversity, Above-ground biomass, Carbon sequestration, Sentinel 2, NDVI

**Cite this article:** Mousivand, T., Azizi, Z., Dehshiri, M.M., Taghavi, L. & Ramezani, M., (2026). Impact of Plant Species Diversity on Aboveground Biomass and Carbon Sequestration in the Peri-Urban Rangelands of North western Tehran, Iran, *Journal of Rangeland Science,* 16(3), 266-277. https://doi.org/10.57647/jrs.2026.1603.24

## 1. Introduction

Urban expansion, particularly in developing megacities, has emerged as a dominant force driving ecological change in the twenty-first century (Angel, 2023). Tehran—especially its northwestern outskirts—exemplifies this trend. Rapid infrastructure development has resulted in severe habitat fragmentation, biodiversity degradation, and ecosystem instability. In such areas, these changes are not merely spatial transformations; they entail profound ecological consequences.Plant species diversity, in particular, is under threat, compromising a range of ecosystem services such as water retention, nutrient cycling, and resilience to climatic stress (Hooper et al., 2012; Klippel et al., 2017; Pordel et al., 2017). The situation in Tehran reflects a broader global concern: as plant biodiversity declines due to urbanization, ecosystems become less capable of regulating essential functions. Reduced species richness weakens ecological

networks, leading to simplified food webs and lower productivity. These shifts directly impair a critical service—carbon sequestration—which relies heavily on the biological and structural complexity provided by diverse plant communities (Grime, 1998; Bakhtiarvand Bakhtiari et al., 2018). Carbon sequestration—the process of capturing and storing atmospheric carbon dioxide—plays a central role in mitigating climate change. Vegetation, especially through its AGB, is a key agent in this process. AGB refers to the total mass of living plant material above the soil, and serves as a primary metric for evaluating carbon storage in ecosystems (Safari and Sohrabi, 2019; Azizi, 2018; Calders et al., 2015). In this study, 'biodiversity' is used strictly to mean plant species diversity; faunal components were not surveyed, and all indices and maps refer to plant communities. Urban sprawl typically results in a decline in vegetative cover and biomass, reducing the carbon sink capacity of a region. In cities like Tehran, where vegetated land is rapidly converted into impermeable surfaces, the reduction in natural carbon storage exacerbates the urban heat island effect and intensifies local climate variability (Haile et al., 2024; Azizi and Miraki, 2024; Klaus and Kiehl, 2021). Plant biodiversity directly influences this process. More diverse plant communities tend to be more productive and efficient at carbon assimilation, as they exhibit functional complementarity—i.e., different species utilize resources in unique and synergistic ways (Grace et al., 2016; Moussa et al., 2019). This interconnection implies that plant biodiversity conservation is not only a matter of ecological preservation but also a climate imperative. Therefore, quantifying how plant diversity affects biomass—and, by extension, carbon sequestration—is vital for developing nature-based strategies in urban and peri-urban areas. There is extensive evidence to support the hypothesis that plant biodiversity enhances carbon storage through increased biomass production. Studies conducted in diverse ecosystems—from temperate forests to rangelands—demonstrate that greater species richness is typically associated with higher levels of primary productivity and carbon retention (Safari and Sohrabi, 2020; Wu et al., 2015; Zhang and Chen, 2015; Hooper et al., 2012). For instance, Reich et al. (2004) showed that species and functional diversity independently contribute to biomass accumulation under elevated $CO_2$ conditions. Likewise, Grace et al. (2016) used integrative modeling to reveal that plant richness indirectly boosts ecosystem productivity by enhancing structural and biogeochemical dynamics. However, the relationship is not universally linear. Some studies have found unimodal or even negative relationships under specific conditions, such as nutrient limitation, water stress, or anthropogenic disturbance (Liang et al., 2016; Laossi et al., 2008). These mixed results underscore the importance of contextual studies, especially in urban regions where such disturbances are intense and variable. In Iran, empirical investigations by Faraji et al. (2022) in Mazandaran's summer pastures confirmed significant correlations between biodiversity indices (e.g., Shannon-Wiener, Simpson) and aboveground biomass. Similarly, Mohammadi et al. (2022) used Generalized Linear Model (GLM) and Boosted Regression Tree (BRT) to predict biodiversity and associated carbon content across various rangeland habitats. These models revealed that certain diversity metrics—such as richness and evenness—could effectively estimate ecosystem-level carbon storage. Other researchers have utilized advanced remote sensing tools to explore biodiversity-carbon relationships at landscape scales. Azizi (2018) demonstrated the utility of terrestrial photogrammetry for estimating biomass in Zagross vegetation, providing benchmarks for similar applications in semi-arid landscapes. The application of remote sensing, particularly using Sentinel-2 imagery, has revolutionized biodiversity and biomass assessments. With its 10–20-meter resolution and spectral bands optimized for vegetation analysis, Sentinel-2 can detect subtle changes in canopy cover and classify land use types with high accuracy (Olofsson et al., 2014). For example, Azizi et al. (2018) demonstrated the utility of terrestrial photogrammetry for estimating biomass in Iranian oak forests, providing benchmarks for similar applications in semi-arid landscapes. In the present study, any city-wide maps are provided solely for contextual reference; all statistical analyses and interpretations are strictly confined to the AOI. These tools are especially useful in urban settings, where field access is often limited. By combining field plots with satellite-derived NDVI, researchers can scale up biomass estimates and monitor vegetation dynamics over time. This integrative approach enables not just accurate quantification, but also trend analysis and policy development. Despite global and regional advances, urban environments in Iran remain underexplored with respect to plant biodiversity–carbon relationships. Tehran's peri-urban fringe—where natural and built environments intersect—is particularly dynamic. The interaction of elevation, land use, and microclimate makes this zone an ideal setting for examining how plant diversity influences ecological function. Nevertheless, the empirical data and resulting inferences of this study are limited to three peri-urban rangeland sites in northwestern Tehran; urban parks and built-up districts were not sampled and therefore fall outside the scope of inference. This study aims to evaluate the impact of plant biodiversity on carbon sequestration in the northwestern margins of Tehran. Specifically, it seeks to: 1) assess

species diversity using indices such as Shannon-Wiener, Simpson, Margalef, Menhinick, Pitt, and Hill; 2) estimate AGB via direct measurement and laboratory analysis; and 3) integrate satellite classification using Sentinel-2 data within the AOI; all statistics and interpretations are confined to these rangeland ecosystems.

## 2. Materials and methods

### 2.1. Study area

The study area is located on the southern foothills of the Alborz Mountains, along the north-western peri-urban fringe of Tehran. Due to its elevation gradient and marked microclimatic heterogeneity, the region is well suited to examining links between plant diversity and biomass in semi-arid rangeland systems. The AOI was delineated as a polygon encompassing only the three sampled sites; all statistical analyses, accuracy assessments and inferences were conducted and reported exclusively within this AOI and were not generalised to urban districts lacking natural vegetation. City-wide and administrative layers were included in the maps solely for contextual visualization. Each sampling site covers approximately 80 ha, giving a cumulative ground-sampled area of 240 ha. Fig 1 illustrates the AOI boundary and its context relative to the wider city.

### 2.2. Field data collection

Field data were collected in 2022 from three ecological plots located in the north-western outskirts of Tehran, Iran (Fig 1). The plots were positioned across the peri-urban rangelands to capture local variation in topography, vegetation structure and land-use intensity, with plot centres at approximately 35.794° N, 51.313° E (Plot 1), 35.800° N, 51.337° E (Plot 2) and 35.807° N, 51.355° E (Plot 3) in WGS84 coordinates. Each plot was delineated in the field using a handheld GPS and characterised in terms of altitude, slope, aspect and dominant land-cover type. This sampling design ensured that both relatively undisturbed rangeland and more degraded, human-impacted vegetation were represented within the sampling framework.

### 2.3. Sampling method

Within each plot, systematic vegetation sampling was carried out using 1 × 1 m quadrats placed at regular intervals to ensure adequate spatial coverage and to minimize sampling bias. In each quadrat, all vascular plant species were recorded, and percentage cover was visually estimated. Species identification was performed either in the field or in the laboratory using regional floristic references to ensure taxonomic consistency. In addition to floristic data, qualitative field observations and georeferenced photographs were collected at each quadrat location to document ground conditions and landscape context. These observations were subsequently used for ecological interpretation and as ground truth for satellite image validation. Above-ground biomass was estimated using the direct harvest method. Within each 1 × 1 m quadrat, all above-ground plant material (shoots and leaves) was clipped at ground level and collected separately for each quadrat. To preserve sample integrity, the harvested material was placed in perforated paper envelopes and transported to the laboratory.

### 2.4. Laboratory analysis

In the laboratory, samples were first carefully washed to remove soil particles and other debris, then air-dried at room temperature. Subsequently, they were oven-dried at 60 °C for 8 hours to remove residual moisture and to obtain a constant dry weight. The dry biomass of each quadrat was determined using a digital balance, and AGB per unit area (g $m^{-2}$) was calculated accordingly.

Organic Matter (OM) content of the biomass was determined using the standard Loss on Ignition (LOI) method. Dried plant material was ground to a fine consistency, and subsamples of 10 g were placed in pre-weighed ceramic crucibles. The crucibles were then combusted in a muffle furnace at 450 °C for 24 hours. After combustion, the crucibles were cooled in a desiccator and reweighed to determine ash weight.

OM was calculated as:

$$\mathrm{OM} = \mathrm{W1} - \mathrm{W2} \quad (1)$$

where: W1 is the dry weight of the sample (g) before combustion, and W2 is the ash weight after combustion (g).

Organic Carbon (OC) content was estimated as:

$$OC = 0{,}54 \times OM \quad (2)$$

(Ortega et al., 2024). This procedure has been widely applied in ecological and soil science studies and has been validated previously for Iranian pasturelands, making it suitable for estimating carbon stocks in natural and semi-natural vegetation.

### 2.5. Biodiversity indices

The floristic data obtained from each 1 × 1 m quadrat were used to compute a suite of biodiversity metrics describing species diversity, richness and evenness. All indices were calculated at the quadrat level and then summarized at the plot scale (Table 2).

#### 2.5.1. *Simpson's diversity index*

Simpson's diversity index ($D$) was calculated using the classical "1 − λ" formulation:

$$D = 1 - \sum_{i=1}^{S} \frac{n_i(n_i-1)}{N(N-1)} \quad (3)$$

Where: values of D approach 0 when one species dominates the community and approach 1 when individuals are more evenly distributed among species.

10.57647/jrs.2026.1603.24

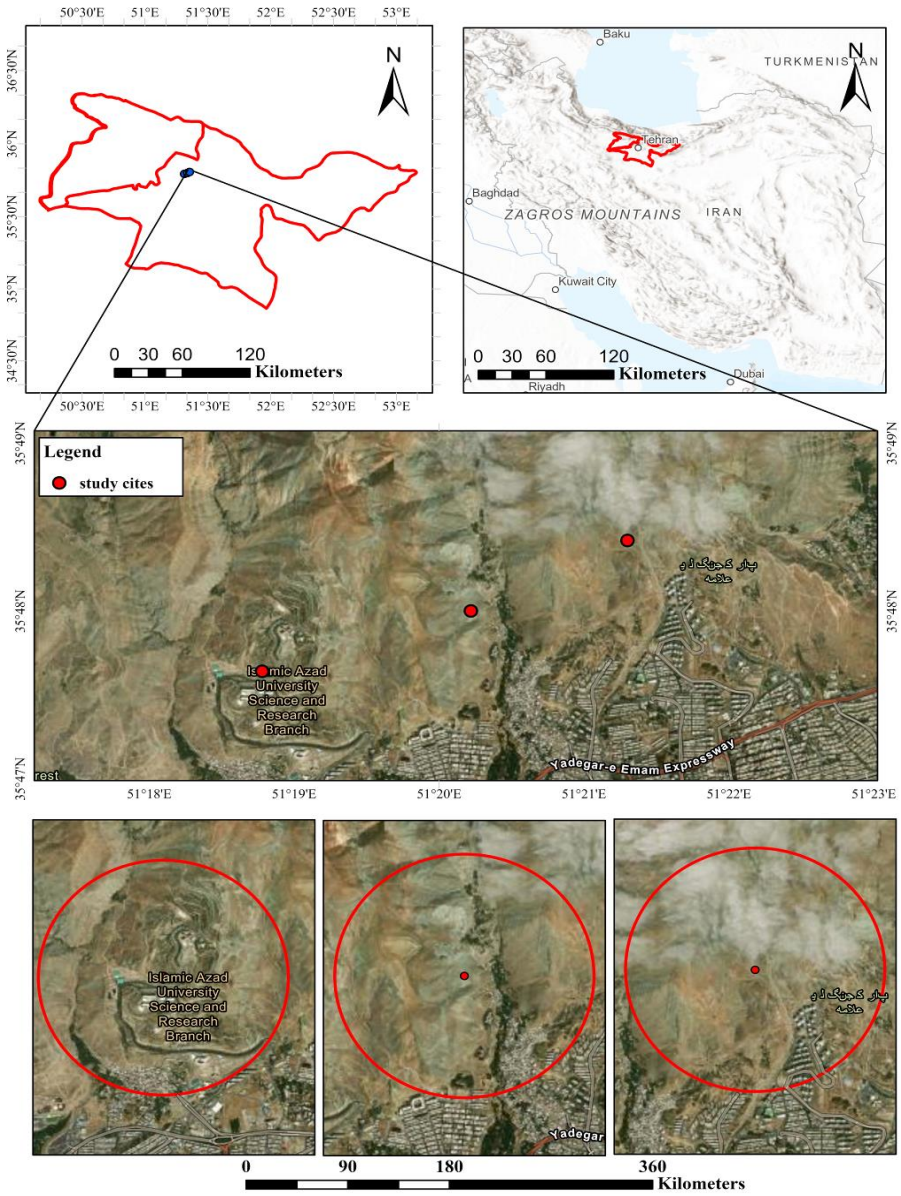


**Figure 1.** The location of the study area

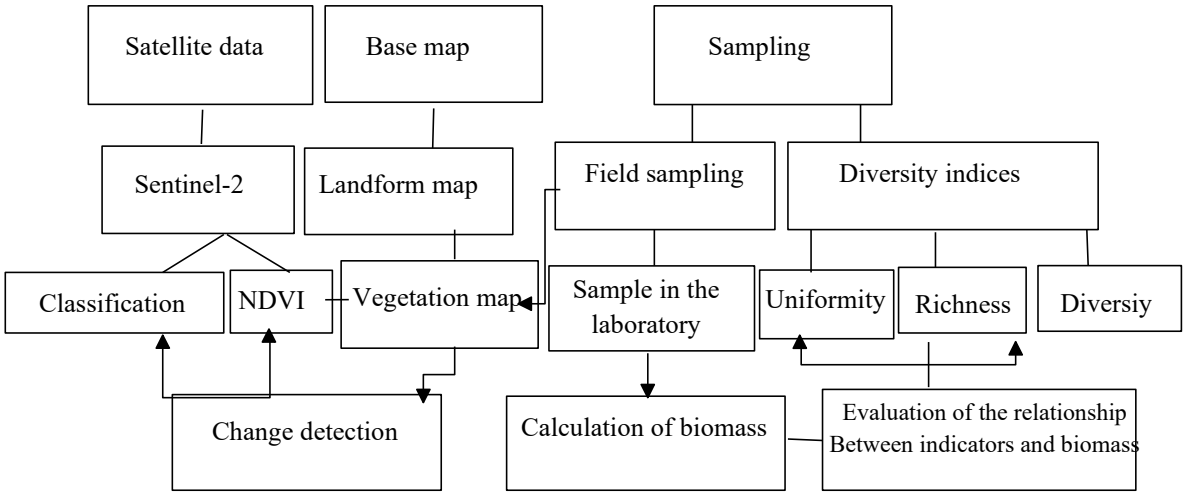


**Figure 2.** Overview of methods used

10.57647/jrs.2026.1603.24

2.5.2. *Shannon–Wiener diversity index*

The Shannon-Wiener index ($H'$) was used as a complementary measure of diversity that incorporates both richness and relative abundance:

$$H' = -\sum_{i=1}^{S} p_i \ln(p_i) \quad (4)$$

Higher values of $H'$indicate a more diverse community with a more even distribution of individuals among species.

2.5.3. *Species richness*

Simple species richness ($S$) was defined as the total number of species recorded in each quadrat and plot, without weighting by abundance:

$$S = \text{number of recorded species} \quad (5)$$

2.5.4. *Margalef richness index*

Margalef's richness index ($R_{\text{Mg}}$) standardizes species richness by the total number of individuals:

$$R_{\text{Mg}} = \frac{S-1}{\ln(N)} \quad (6)$$

This index increases with greater species richness for a given sample size.

2.5.5. *Menhinick richness index*

Menhinick's richness index ($R_{\text{Mn}}$) relates the number of species to the square root of the total number of individuals:

$$R_{\text{Mn}} = \frac{S}{\sqrt{N}} \quad (7)$$

Larger values of $R_{\text{Mn}}$indicate higher richness relative to the number of individuals sampled.

2.5.6. *Pielou (Pitt) evenness index*

Evenness was quantified using Pielou's (Pitt) evenness index ($E$), which normalises Shannon diversity by the maximum possible value for a given richness:

$$E = \frac{H'}{\ln(S)} \quad (8)$$

Values of $E$range from 0 to 1, with values closer to 1 indicating a more even distribution of individuals among species.

2.5.7. *Hill diversity index*

To provide an additional, abundance-sensitive measure of diversity, Hill's second diversity number ($N_2$) was also calculated

$$N_2 = \frac{1}{\sum_{i=1}^{S} p_i^2} \quad (9)$$

Higher values of $N_2$correspond to communities where dominance is low and individuals are more evenly distributed across species.

For all indices, the following notation was used:

$S$: Total number of species in the sample (species richness)

$N$: Total number of individuals (all species combined)

$n_i$: Number of individuals belonging to species $i$

$p_i$: Relative abundance of species$i$, defined as $p_i = \frac{n_i}{N}$

$H'$: Shannon–Wiener diversity index

ln : Natural logarithm.

All these indices (Simpson, Shannon–Wiener, species richness, Margalef, Menhinick, Pielou's evenness and Hill's diversity) provide a comprehensive description of plant community structure in the three study plots and were subsequently related to AGB and carbon content.

**2.6. Statistical analysis**

To explore relationships between vegetation structure, diversity and carbon storage, Pearson correlation analyses were performed between above-ground biomass, organic carbon and the calculated diversity, richness and evenness indices.

All descriptive statistics and correlation analyses were conducted using standard statistical software (fig 2).

**2.7. Remote-sensing methods**

2.7.1. *Sentinel-2 data acquisition*

Vegetation change over time was assessed using Sentinel-2 satellite imagery acquired for July 2018 and July 2022. Sentinel-2 is part of the European Space Agency's Copernicus program and consists of two identical satellites, Sentinel-2A and Sentinel-2B, each carrying a Multi-spectral Instrument (MSI) with 13 spectral bands. These bands include:

- 10 m spatial resolution: visible bands (B2 – Blue, B3 – Green, B4 – Red) and near-infrared (B8);
- 20 m spatial resolution: red-edge bands (B5, B6, B7, B8A) and short-wave infrared (SWIR) bands (B11, B12);
- 60 m spatial resolution: coastal aerosol (B1) and cirrus (B10).

These spectral and spatial characteristics make Sentinel-2 particularly suitable for vegetation mapping and land-use/land-cover (LULC) analysis in heterogeneous peri-urban landscapes such as northwestern Tehran (Fig 1).

2.7.2. *Image pre-processing*

Level-1C Sentinel-2 products were first atmospherically corrected to surface reflectance. Images were then subset to the study area and visually inspected to avoid cloud contamination. When necessary, cloud-affected pixels and shadows were masked using standard quality layers. All bands required for vegetation indices and classification were co-registered and resampled to a common 10 m spatial resolution to ensure pixel-wise comparability between dates and spectral layers.

2.7.3. *NDVI calculation and vegetation mapping*

The NDVI was calculated for both 2018 and 2022 images using the red (B4) and near-infrared (B8) bands:

$$NDVI = \frac{NIR-Red}{NIR+Red} \quad (10)$$

Where $NIR$ and $Red$ denote the reflectance values in bands B8 and B4, respectively. NDVI maps were used to characterise the spatial distribution and relative vigor of vegetation in the study area for the two dates. Thresholds and NDVI ranges were interpreted in combination with field observations and high-resolution imagery to distinguish vegetated and non-vegetated surfaces.

2.7.4. *Supervised land-cover classification (Maximum Likelihood)*

To produce detailed land-cover maps and quantify changes in vegetation, a supervised classification was performed on the Sentinel-2 images using the MLC algorithm. Training data were derived from two sources:

1) The three field plots, where vegetation and ground conditions were documented in detail, and
2) Additional training sites were manually delineated across the region using high-resolution Google Earth imagery.

Training polygons were defined for the main land-cover classes (e.g. dense vegetation, sparse vegetation, built-up areas, and bare soil). Spectral statistics for each class were extracted from the selected Sentinel-2 bands and used as input to the MLC classifier. The resulting classified maps for 2018 and 2022 provided a spatially explicit description of vegetation and land-use patterns in and around the study area (Fig 2).

2.7.5. *Accuracy assessment and change-detection analysis*

Classification accuracy was evaluated using an independent set of validation points drawn from both field observations and visually interpreted high-resolution imagery. A confusion matrix was generated for each year, and standard accuracy metrics, including overall accuracy, producers' and users' accuracy for individual classes, and the kappa coefficient, were calculated. High overall accuracy and strong kappa values indicated that the MLC approach performed robustly, despite the limited number of ground plots. To quantify temporal changes, post-classification comparison was applied to the 2018 and 2022 land-cover maps. Transitions between vegetated and non-vegetated classes were computed on a pixel-by-pixel basis to estimate net gains and losses in vegetation cover across the study area (Habibi Razi and Azizi, 2023). These changes in vegetation extent were then interpreted together with field-based estimates of biomass and carbon to assess the carbon sequestration capacity of the peri-urban vegetation over the study period.

## 3. Result

### 3.1. Field-based vegetation patterns and above-ground biomass

Field sampling across the three peri-urban rangeland plots yielded 1,558 individual plant specimens, representing 38 morphological types and 31 identified species. Species composition and abundance showed clear spatial variation among sites. In Plot 1, located on the north-western fringe of Tehran, 506 individuals were recorded; *Astracantha gossypina* and *Ferula elbursensis* were the most frequent and spatially extensive species. Plot 2 contained 497 individuals, again representing 38 main plant types; *Eremurus luteus* and *Taraxacum nouveau* dominated this site, while *Heteranthelium piliferum*, *Ceratocephalus falcatus* and *Melica persica* occurred only sparsely. Plot 3 supported 555 individuals, with *Ceratocephalus falcatus* and *Poa bulbosa* showing high abundance, whereas *Stipa ehrenbergiana* and *Onosma ghahremanii* were restricted to a few quadrats. AGB varied markedly among vegetation types (Table 1). The highest biomass was associated with the *Psathyrostachys* type (23 kg ha$^{-1}$), followed by *Ferula–Onosma* (16 kg ha$^{-1}$) and *Minuartia* and *Melica* (12 and 11 kg ha$^{-1}$, respectively). Several mixed associations, including *Ferula–Psathyrostachys*, *Festuca–Ferula*, *Psathyrostachys–Festuca* and *Ferula–Stipa*, showed intermediate biomass values (5–10 kg ha$^{-1}$), whereas *Bromus*, *Galium*, *Heteranthera* and *Verbascum* exhibited the lowest biomass (< 3 kg ha$^{-1}$). When vegetation types were summarized at the community level, mean species richness, biomass, plant abundance (number of quadrats) and vegetation cover also differed substantially (Table 2). For example, the *Stipa* and *Astragalus–Stipa* associations were the most spatially extensive (24 and 22 quadrats, respectively) but had moderate biomass (3–4 kg ha$^{-1}$), whereas *Psathyrostachys*, *Psathyrostachys–Festuca* and *Ferula–Onosma* combined relatively high biomass with moderate to high vegetation cover (21–29%). These contrasts indicate that both dominant grasses and forb–shrub mixtures contribute to the overall biomass pool, albeit through different combinations of areal extent, species richness and local productivity.

### 3.2. Relationships between plant diversity and biomass

Pearson correlation analysis revealed consistent positive relationships between terrestrial biomass and several diversity, richness and evenness indices (Table 3). Shannon–Wiener diversity showed the strongest association with AGB ($r = 0.63$, $p<0.01$), followed by Simpson's index ($r = 0.41$, $p<0.05$). Richness-oriented metrics also correlated positively with biomass: Margalef ($r = 0.46$, $p<0.05$) and Menhinick ($r = 0.44$, $p<0.05$)

indices both indicated that quadrats with higher species richness tended to support greater biomass.

**Table 1**. Scientific names of plant species identified in the study sites and above-ground biomass measured for each species (kg ha$^{-1}$)

| Row | Dominant species/association | Biomass (kgha$^{-1}$) | Row | Dominant species/association | Biomass (kgha$^{-1}$) |
|---|---|---|---|---|---|
| 1 | *Psathyrostachys* | 23 | 20 | *Cousinia* | 6 |
| 2 | *Ferula–Onosma* | 16 | 21 | *Stipa–Psathyrostachys* | 5 |
| 3 | *Minuartia* | 12 | 22 | *Poa bulbosa* | 5 |
| 4 | *Melica* | 11 | 23 | *Eremurus* | 5 |
| 5 | *Noaea* | 11 | 24 | *Ferula–Stipa* | 5 |
| 6 | *Adonis* | 10 | 25 | *Agropyron* | 5 |
| 7 | *Ferula–Psathyrostachys* | 10 | 26 | *Lactuca* | 5 |
| 8 | *Artemisia* | 9 | 27 | *Astragalus–Stipa* | 4 |
| 9 | *Eryngium* | 9 | 28 | *Aethionema–Psathyrostachys* | 4 |
| 10 | *Thymus praecox* | 9 | 29 | *Boissiera* | 4 |
| 11 | *Euphorbia* | 7 | 30 | *Astracantha* | 4 |
| 12 | *Alyssum* | 7 | 31 | *Astragalus* | 3 |
| 13 | *Henrardia* | 6 | 32 | *Stipa–Onosma* | 3 |
| 14 | *Elymus* | 6 | 33 | *Stipa* | 3 |
| 15 | *Aethionema–Stipa* | 6 | 34 | *Taraxacum* | 3 |
| 16 | *Phlomis* | 6 | 35 | *Bromus* | 2 |
| 17 | *Ceratocephalus* | 6 | 36 | *Galium* | 2 |
| 18 | *Psathyrostachys–Festuca* | 6 | 37 | *Heteranthera* | 2 |
| 19 | *Festuca–Ferula* | 6 | 38 | *Verbascum* | 1 |

**Table 2.** Vegetation types (dominant species/associations) with plant diversity (mean species richness), above-ground biomass, plant abundance (number of quadrats) and mean vegetation cover

| Vegetation type (dominant species/association) | Plant diversity (species richness /quadrat) | Biomass (kg ha$^{-1}$) | Abundance of plant species (no. of quadrats)* | Vegetation cover (%) |
|---|---|---|---|---|
| *Aethionema–Psathyrostachys* | 10.0 | 4 | 2 | 25 |
| *Aethionema–Stipa* | 11.0 | 6 | 2 | 25 |
| *Astragalus* | 6.0 | 3 | 1 | 18 |
| *Astragalus–Stipa* | 7.9 | 4 | 22 | 20 |
| *Ferula–Onosma* | 11.0 | 16 | 1 | 25 |
| *Ferula–Psathyrostachys* | 11.0 | 10 | 1 | 25 |
| *Ferula–Stipa* | 6.0 | 5 | 1 | 17 |
| *Festuca–Ferula* | 9.0 | 6 | 1 | 13 |
| *Psathyrostachys* | 8.5 | 23 | 12 | 21.2 |
| *Psathyrostachys–Festuca* | 8.0 | 6 | 1 | 29.0 |
| *Stipa* | 7.4 | 3 | 24 | 18.0 |
| *Stipa–Onosma* | 8.0 | 3 | 1 | 20.0 |
| *Stipa–Psathyrostachys* | 7.5 | 5 | 13 | 21.2 |

**Table 3.** Pearson's correlation test results of richness and evenness indices with terrestrial biomass

| Biodiversity indices | Diversity values (r) |
|---|---|
| Margalef index | 0.46* |
| Menhinick index | 0.44* |
| Pit index | 0.41* |
| Hill index | $-0.24^{ns}$ |
| Simpson index | 0.41* |
| Shannon–Wiener index | 0.63** |

ns = non-significant; *, **= significant at 5% and 1% probability level, respectively

10.57647/jrs.2026.1603.24

Pielou's (Pitt) evenness index exhibited a significant positive correlation with biomass as well ($r = 0.41$, $p<0.05$), suggesting that communities in which individuals are more evenly distributed among species are also more productive. In contrast, Hill's diversity number showed a negative but non-significant correlation ($r = -0.24$, $p>0.05$), implying that this particular metric is less sensitive to biomass variation in the studied semi-arid rangelands. Collectively, these results support the hypothesis that species-rich and structurally even plant communities store more above-ground biomass and, by inference, more organic carbon.

### 3.3. Patterns of diversity, biomass and abundance

Synthesising the plot-level floristic and biomass data at the scale of vegetation types highlighted how local diversity translates into broader community characteristics (Table 2). The *Aethionema–Stipa* and *Aethionema–Psathyrostachys* relations exhibited the highest mean species richness per quadrat (≈10–11 species), high vegetation cover (~25%) and moderate biomass (4–6 kg ha$^{-1}$), indicating structurally complex but not necessarily highly productive stands. In contrast, the *Psathyrostachys* relation combined relatively high biomass (23 kg ha$^{-1}$) with moderate richness (8.5 species per quadrat) and extensive areal coverage (12 quadrats). The widely distributed *Stipa* and *Stipa–Psathyrostachys* types also showed intermediate richness (7.4–7.5 species) and biomass (3–5 kg ha$^{-1}$), but together accounted for 37 quadrats, underscoring their importance for landscape-scale carbon storage. Vegetation types with limited spatial extent, such as *Ferula–Onosma*, *Ferula–Psathyrostachys* and *Festuca–Ferula*, nonetheless contributed disproportionately high biomass and vegetation cover within their respective quadrats. These combined patterns indicated that both dominant, widespread grasslands and locally restricted forb–shrub communities play complementary roles in maintaining biodiversity and biomass in the peri-urban rangelands.

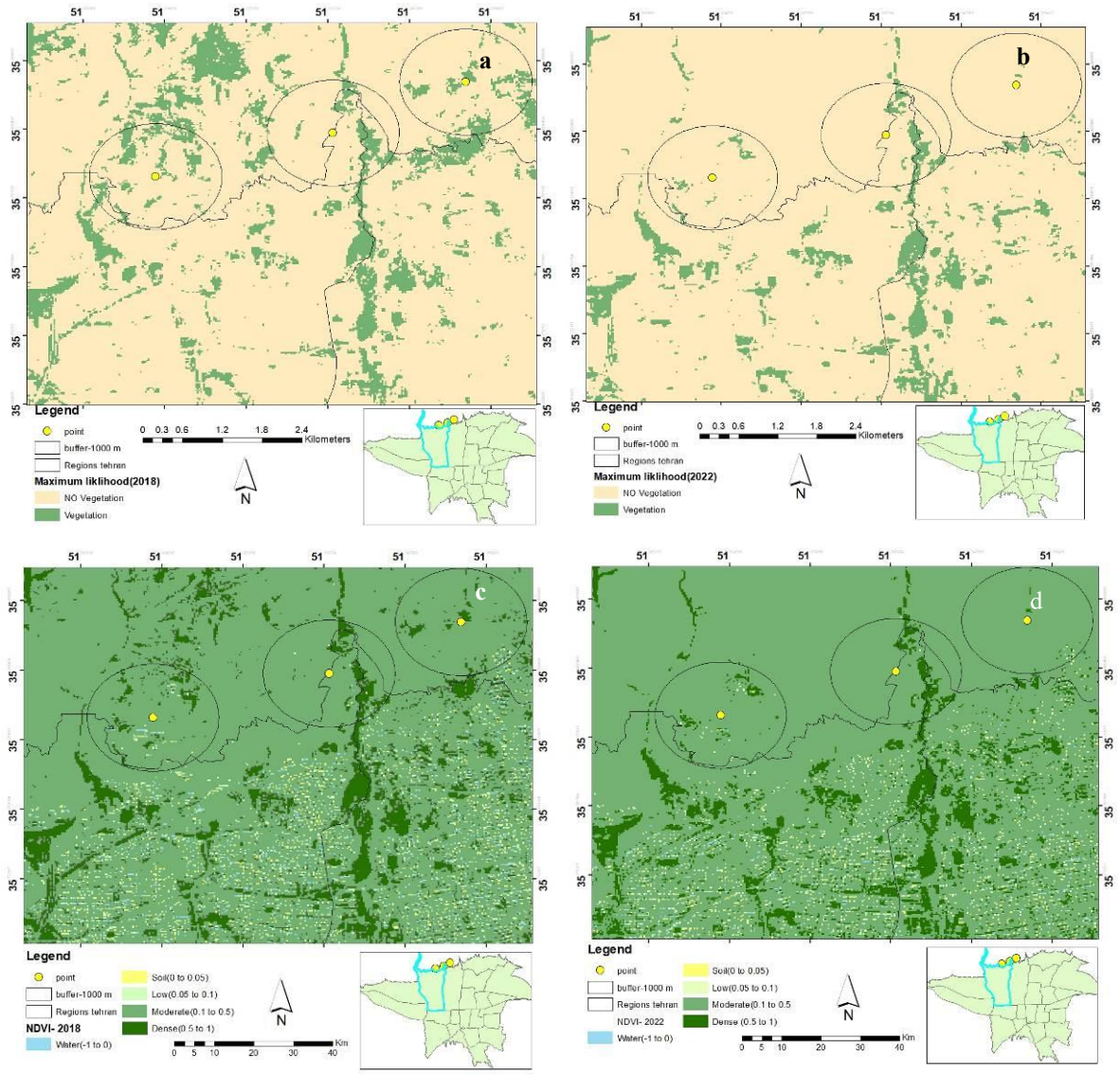


**Figure 3.** a, b) Classification of Maximum Likelihood (2018) and (2022) c, d) Vegetation map (NDVI) (2018, 2022)

**Table 4.** Accuracy assessment and class-change statistics derived from Sentinel-2 MLC (2018–2022)

(a) Confusion matrix and accuracy indices for 2018 classification

| Land use (reference) | Vegetation | Non-vegetation | Total | User's accuracy (commission error) |
|---|---|---|---|---|
| Vegetation | 92 | 0 | 92 | 92 / 92 |
| Non-vegetation | 1 | 200 | 201 | 200 / 201 |
| Total | 93 | 200 | 293 | – |

Overall accuracy = 99.65%, Kappa coefficient = 99.00%

(b) Confusion matrix and accuracy indices for 2022 classification

| Land use (reference) | Vegetation | Non-vegetation | Total | User's accuracy (commission error) |
|---|---|---|---|---|
| Vegetation | 2 | 320 | 322 | 0 / 320 |
| Non-vegetation | 135 | 0 | 135 | 2 / 137 |
| Total | 137 | 320 | 457 | – |

Overall accuracy = 99.56%, Kappa coefficient = 95.00%

(c) Matrix class changes by percent (2018–2022)

| 2018 → 2022 | Non-vegetation (%) | Vegetation (%) |
|---|---|---|
| Non-vegetation | 96.51 | 3.49 |
| Vegetation | 34.97 | 65.02 |
| Class changes | 3.49 | 34.97 |
| Image difference | 1.041 | −8.035 |

### 3.4. Remote-sensing classification accuracy and vegetation-cover changes

The supervised MLC applied to Sentinel-2 images produced highly accurate land-cover maps for both 2018 and 2022 (Fig 3a-b; Table 4a–b). For the 2018 classification, the confusion matrix indicated that 92 of 93 vegetation reference samples and 200 of 201 non-vegetation samples were correctly classified, yielding producers' accuracies of 92/93 (99.0%) and 200/201 (99.5%), respectively. The overall accuracy reached 99.65%, with a Kappa coefficient of 99.0%, indicating near-perfect agreement between the classified map and the reference data. In 2022, 135 of 137 vegetation pixels and all 320 non-vegetation pixels were correctly assigned, corresponding to producers' accuracies of 135/137 (98.5%) and 320/320 (100%). Overall accuracy remained high at 99.56%, with a Kappa coefficient of 95.0%. The slight reduction in Kappa between years reflects increased spectral confusion at some vegetation–non-vegetation boundaries rather than systematic misclassification.

Post-classification comparison of the 2018 and 2022 maps demonstrated marked temporal dynamics in vegetation cover (Fig 3c–d; Table 4c). Of the area classified as vegetation in 2018, 65.02% remained vegetated in 2022, whereas 34.97% transitioned to non-vegetation, indicating substantial loss or degradation of vegetated surfaces within the AOI. In contrast, 96.51% of 2018 non-vegetation remained stable, with only 3.49% converting to vegetation. The "image difference" row in Table 4c shows a net increase of approximately 1.041% in non-vegetation and a corresponding 8.035% decline in vegetation over the five-year period. These changes are consistent with ongoing urban expansion and land-use intensification in the north-western fringe of Tehran and, when interpreted alongside the field-based biomass and diversity metrics, underscore the vulnerability of carbon-rich, species-diverse rangeland patches to peri-urban development pressures.

## 4. Discussion

Plant diversity and aboveground biomass are foundational elements of ecosystem functioning, directly influencing productivity, resilience, and services such as carbon sequestration. In recent years, the relationship between plant species diversity and biomass accumulation has gained increased attention, particularly in the context of global environmental changes and urban expansion (Cardinale et al., 2012; Isbell et al., 2017). Plant diversity enhances ecosystem multifunctionality through mechanisms like niche complementarity, facilitation, and trait variability (Loreau and Hector, 2001; Tilman et al., 2012). Our findings revealed a significant positive correlation between plant diversity indices and aboveground biomass in the northwestern fringes of Tehran. Specifically, indices such as Simpson, Shannon-Wiener, Margalef, Menhinick, and Pitt displayed strong associations with increased biomass levels. This supported the hypothesis that species-rich communities are more productive due to complementary resource use and enhanced ecological efficiency (Guo et al., 2010; Zhang and Chen, 2015). However, not all evenness

measures followed this pattern; for example, the Hill index showed no significant correlation with biomass, highlighting index-specific sensitivity to community structure. The observed results align with several large-scale experiments and meta-analyses conducted in grassland and forest ecosystems worldwide. For instance, studies by Hooper et al. (2012) and Tilman et al. (2012) demonstrated that high species richness tends to stabilize ecosystem processes and boost productivity. Similarly, Liang et al. (2016) found a positive biodiversity–productivity relationship across global forests. In contrast, Reich et al. (2004) and Grace et al. (2016) reported context-dependent or even inverse relationships, emphasizing the need for site-specific ecological assessments.

Urban-rural ecotones, such as our study area, present unique challenges due to land-use fragmentation, pollution, and microclimatic variability. These factors can lead to non-linear and spatially heterogeneous plant biodiversity–biomass patterns (Niemelä, 1999; Aronson et al., 2014). Nevertheless, our study confirmed that even in disturbed or transitional urban areas, preserving plant diversity supports higher biomass accumulation and potentially greater carbon sequestration. In line with our findings, recent research by Haile et al. (2024) underscored the importance of functional diversity in determining ecosystem service delivery. Functional traits such as growth form, leaf area index, and phenology can modulate the effect of diversity on productivity. Our field observations and biomass data suggest that dominant species with favorable functional traits, such as those in the Bromus and Festuca groups, contribute substantially to total biomass. This highlights the dual role of species richness and trait-based dominance in shaping urban vegetation structure.

Moreover, our use of Sentinel-2 imagery and MLC proved effective for vegetation mapping. The overall accuracies of 99.65% (2018) and 99.56% (2022), with Kappa coefficients of 99% and 95%, respectively, indicated that remotely sensed data, when combined with targeted ground-truthing, can provide reliable insights into land cover dynamics. The observed 34% change in vegetation cover over five years underscored the rapid pace of ecological transformation in peri-urban landscapes.The correlation between plant diversity and carbon sequestration in this context is further validated by studies like Klaus and Kiehl (2021), who demonstrated that floristically rich meadows stored more soil and biomass carbon than monocultures. Similarly, Mohammadi et al. (2022) used statistical modeling to link species diversity with organic carbon stocks in Iranian rangelands, reinforcing the relevance of our findings. Despite these insights, certain limitations remain. For example, while biomass was directly measured and linked to diversity indices, other factors such as soil fertility, water availability, and human disturbance were not fully controlled. Future studies should incorporate these variables and expand to include functional trait databases and phylogenetic diversity metrics to better understand the multidimensional role of biodiversity in urban ecosystem services (Cadotte et al., 2011).

## 5. Conclusion

This study highlights the pivotal role of plant biodiversity in supporting aboveground biomass accumulation and, consequently, carbon sequestration in the peri-urban landscapes of northwestern Tehran. By integrating rigorous field sampling, standardized laboratory analyses, and advanced satellite-based methods, the research provides robust empirical evidence that diverse plant communities make a substantial contribution to ecosystem productivity. The findings carry significant implications for urban sustainability and ecological planning.Within the studied rangelands, maintaining or enhancing plant species diversity could support carbon-oriented nature-based solutions, such as assisted regeneration or diversified seeding mixes that stabilize biomass under variable rainfall. For urban planning, the results underscore the potential of peri-urban buffers to deliver climate co-benefits; however, these implications are specific to peri-urban rangelands and should not be generalized to Tehran's built-up districts without further sampling. Linking species composition and ecological structure to measurable carbon outcomes provides a practical framework for policymakers and urban ecologists seeking to mitigate climate impacts through nature-based approaches. In summary, this study demonstrates that urban biodiversity is not merely an ecological asset but a strategic component of climate mitigation and sustainable development. By safeguarding and promoting plant diversity, cities can enhance both environmental performance and quality of life for future generations.

## Acknowledgment

The authors gratefully acknowledge the financial support for this work that was provided by the University.

**Authors Contribution**
Authors have contributed equally in preparing and writing the manuscript.

**Availability of data and materials**
The data that support the findings of this study are available on request from the corresponding author.

**Conflict of interests**
I certify that there is no actual or potential conflict of interest concerning this article.

## References


Angel, S., 2023. Urban expansion: theory, evidence, and practice. Buildings and Cities, 4(1), 124–138.

Aronson, M.F.J., La Sorte, F.A., Nilon, C.H., Katti, M., Goddard, M.A., Lepczyk, C.A., Warren, P.S., Williams, N.S.G., Cilliers, S., Clarkson, B., Dobbs, C., Dolan, R.W., Hedblom, M., Klotz, S., Kooijmans, J.L., Kühn, I., MacGregor-Fors, I., McDonnell, M., Mörtberg, U., Pyšek, P., Siebert, S., Sushinsky, J., Werner, P., Winter, M., 2014. A global analysis of the impacts of urbanization on bird and plant diversity. Proceedings of the Royal Society B, 281(1780), 20133330.

Azizi, Z., 2018. Estimating crown biomass of oak trees using terrestrial photogrammetry in Zagros Forests. In: Conference of the Arabian Journal of Geosciences, pp. 167–169.

Azizi, Z., Miraki, M., 2024. Individual urban tree detection based on point clouds derived from UAV-RGB imagery and local maxima algorithm: a case study of Fateh Garden, Iran. Environment, Development and Sustainability, 2331–2344.

Bakhtiarvand Bakhtiari, S., Sohrabi, H., 2018. Preliminary results of using the random branch sampling method to estimate the biomass of aerial organs of hand-planted mulberry and acacia trees in the Foulad Mubarakeh area. Iran Forest and Spruce Research, 19(4), 571–562. (In Persian).

Cadotte, M.W., Carscadden, K., Mirotchnick, N., 2011. Beyond species: functional diversity and the maintenance of ecological processes and services. Journal of Applied Ecology, 48(5), 1079–1087.

Calders, K., Newnham, G., Burt, A., Murphy, S., Raumonen, P., 2015. Nondestructive estimates of above-ground biomass using terrestrial laser scanning. Methods in Ecology and Evolution, 6, 198–208.

Cardinale, B.J., Duffy, J.E., Gonzalez, A., Hooper, D.U., Perrings, C., Venail, P., Narwani, A., Mace, G.M., Tilman, D., Wardle, D.A., Kinzig, A.P., Daily, G.C., Loreau, M., Grace, J.B., Larigauderie, A., Srivastava, D.S., Naeem, S., 2012. Biodiversity loss and its impact on humanity. Nature, 486(7401), 59–67.

Faraji, A., Tatian, M., Tamertash, R., Sanai, A., 2022. The effect of grazing management on indicators of species and functional diversity of rangeland and the relationship between them on aboveground biomass. Journal of Environmental Science Studies, 7(4), 5696–5710. (In Persian).

Grace, J.B., Anderson, T.M., Seabloom, E.W., Borer, E.T., Adler, P.B., Harpole, W.S., Hautier, Y., Hillebrand, H., Lind, E.M., Pärtel, M., Bakker, J.D., Buckley, Y.M., Crawley, M.J., Damschen, E.I., Davies, K.F., Fay, P.A., Firn, J., Gruner, D.S., Hector, A., Knops, J.M.H., MacDougall, A.S., Melbourne, B.A., Morgan, J.W., Orrock, J.L., Prober, S.M., Smith, M.D., 2016. Integrative modelling reveals mechanisms linking productivity and plant species richness. Nature, 529, 390–393.

Grime, J.P., 1998. Benefits of plant diversity to ecosystems: immediate, filter and founder effects. Journal of Ecology, 86, 902–910.

Guo, M., Zhen, F.L., An, S.S., Liu, Y., An, J., 2010. Dynamic change of soil organic carbon density and microbial biomass carbon during natural revegetation. Journal of Soil and Water Conservation, 24(1), 229–238.

Habibi Razi, A., Azizi, Z., 2023. Object-based and pixel-based methods in land cover change detection using Landsat and WorldView imagery (case study: west of Tehran). Geographical Research, 38(2), 181–190. (In Persian).

Haile, A.A., Seid, A., Mekonnen, A.B., Adnew, W., Yemata, G., Yihune, Mekuriaw, E.A., 2024. Estimation of carbon stocks of woody plant species in church forests of West Gojjam zone, northwestern Ethiopia: implications for climate change mitigation. Trees, Forests and People, 18, 100704.

Hooper, D.U., Adair, E.C., Cardinale, B.J., Byrnes, J.E.K., Hungate, B.A., Matulich, K.L., Gonzalez, A., Duffy, J.E., Gamfeldt, L., O'Connor, M.I., 2012. A global synthesis reveals biodiversity loss as a major driver of ecosystem change. Nature, 486, 105–108.

Isbell, F., Adler, P.R., Eisenhauer, N., Fornara, D., Kimmel, K., Kremen, C., Letourneau, D.K., Liebman, M., Polley, H.W., Quijas, S., Scherer-Lorenzen, M., 2017. Benefits of increasing plant diversity in sustainable agroecosystems. Journal of Ecology, 105(4), 871–879.

Klippel, L., Krusic, P.J., Brandes, R., Hartl-Meier, C., Trouet, V., Meko, M., Esper, J., 2017. High-elevation inter-site differences in Mount Smolikas tree-ring width data. Dendrochronologia, 44, 164–173.

Klaus, V.H., Kiehl, K., 2021. A conceptual framework for urban ecological restoration and rehabilitation. Basic and Applied Ecology, 52, 82–94.

Laossi, K.R., Barot, S., Carvalho, D., Desjardins, T., Lavelle, P., Martins, M., Mitja, D., Rendeiro, A.C., Roussin, J., Sarrazin, M., Velasquez, E., Grimaldi, M., 2008. Effects of plant diversity on plant biomass production and soil macrofauna in Amazonian pastures. Pedobiologia, 51, 397–407.

Loreau, M., Hector, A., 2001. Partitioning selection and complementarity in biodiversity experiments. Nature, 412(6842), 72–76.

Liang, J., Crowther, T.W., Picard, N., Wiser, S., Zhou, M., Alberti, G., Schulze, E.D., et al. 2016. Positive biodiversity–productivity relationship predominant in global forests. Science, 354, 196–210.

Mohammadi, M., Jafarian, Z., Tamartash, R., Kargar, M., 2022. Prediction of plant species biodiversity using Generalized Linear Model (GLM) and Boosted Regression Tree (BRT) in eastern rangelands of Mazandaran. Journal of Rangeland, 16(3), 468–480. (In Persian).

Moussa, S., Kyereh, B., Tougiani, A., Kuyah, S., Saadou, M., 2019. West African Sahelian cities as source of carbon stocks: evidence from Niger. Sustainable Cities and Society, 50, 101653.

Niemelä, J., 1999. Ecology and urban planning. Biodiversity and Conservation, 8(1), 119–131.

Pordel, F., Ebrahimi, A.A., Azizi, Z., 2017. Evaluating spatio-temporal phytomass changes using vegetation index derived from Landsat 8 (case study: Mrajan rangeland, Boroujen). Journal of Rangeland, 2, 166–178. (In Persian).

Reich, P.B., Tilman, D., Naeem, S., Ellsworth, D.S., Knops, J., Craine, J., Wedin, D., Trost, J., 2004. Species and functional group diversity independently influence biomass accumulation and its response to CO2 and N. Proceedings of the National Academy of Sciences of the USA, 101(27), 10101–10106.

Olofsson, P., Foody, G.M., Herold, M., Stehman, S.V., Woodcock, C.E., Wulder, M.A., 2014. Good practices for estimating area and assessing accuracy of land change. Remote Sensing of Environment, 148, 42–57.

Ortega, J.P., Cambronero, L., Alcarria Salas, M., Rodríguez, J.L., Durán-Zuazo, V.H., Keesstra, S.D., Rodrigo-Comino, J., 2024. Conducting an in-situ evaluation of erodibility in a Mediterranean semi-arid and conventional vineyard in Granada province (southern Spain) through rainfall simulation experiments. Euro-Mediterranean Journal for Environmental Integration, 9, 797–808.

Safari, A., Sohrabi, H., 2019. Effect of climate change and local management on aboveground carbon dynamics (1987–2015) in Zagros oak forests using Landsat time-series imagery. Applied Geography, 110, 102048.

Safari, A., Sohrabi, H., 2020. Integration of Synthetic Aperture Radar and multispectral data for aboveground biomass retrieval in Zagros oak forests, Iran: an attempt on Sentinel imagery. International Journal of Remote Sensing, 41, 8069–8095.

Tilman, D., Reich, P.B., Isbell, F., 2012. Biodiversity impacts ecosystem productivity as much as resources, disturbance, or herbivory. Proceedings of the National Academy of Sciences of the United States of America, 109(26), 10394–10397.

Wu, X., Wang, X.P., Tang, Z.Y., Shen, Z.H., Zheng, C.Y., Xia, X.L., Fang, J.Y., 2015. The relationship between species richness and biomass changes from boreal to subtropical forests in China. Ecography, 38(6), 602–613.

Zhang, Y., Chen, H.Y.H., 2015. Individual size inequality links forest diversity and above-ground biomass. Journal of Ecology, 103, 1245–1252.

10.57647/jrs.2026.1603.24